International Journal of Geology and Earth Sciences

ISSN 2395-647X www.ijges.com
Vol. 5, No. 1, March 2019
doi:10.32937/IJGES.5.1.2019.21-40

Research Paper

Aerogeophysical Mapping and Evaluation of the Banded Iron Formation (BIF) Occurrence in Birnin Gwari, Northwestern Nigeria

M. U. OHWO[1]*, A. H. Falade[2], Prof. A. A. Adepelumi[3] and Prof. G. O. Asuen[4]

Corresponding Author: **M. U. Ohwo ✉ moses.ohwo@physci.uniben.edu*

Received on: 4th December, 2018 Accepted on: 15th January, 2019

Analyses of aeromagnetic data were carried out in this study to explore the iron ore deposition, delineate the structural settings and estimate the tonnage of iron ore reserve in Birnin Gwari region of Northwestern Nigeria. The data, which covers latitudes 11° 00' N % 11° 30' N and longitudes 6° 30' E% 7° 00' E, was acquired from the Nigeria Geological Survey (NGSA). The aeromagnetic data was filtered using reduction to the equator and upward continuation filters to accentuate anomalies of interest. The resulted filtered residual map showed closely spaced linear sub-parallel orientation of contours at the central portion of the study area, which suggests the possibility of faults and folds passing through the area. Structural analysis was carried on the filtered residual map, using First Vertical Derivative (FVD) and Horizontal Gradient Magnitude (HGM) filtering techniques, to map out geologic linear structures. The inferred lineament map and its rose diagram revealed that the study area is characterized by geologic linear structures that trends in ENE-WSW, NE-SW, WNW-ESE, NW-SE and NNW-SSE directions, with the ENE-WSW trend dominating. Delineation of suspected Banded Iron Formation (BIF) from other magnetic anomalies was achieved using apparent susceptibility filter and pseudogravity transformation. The resulted maps showed anomalous highs, in an approximately N-S direction, along the suspected BIF. Depth analysis, using the Source Parameter Imaging (SPI) technique, revealed that the depth to the magnetic basement across the area varies between 119 and 1304 m. The region around the suspected BIF is characterized by shallow sources (<300 m) surrounded by deep seated sources (>400 m), which suggests that the iron ore mineralization has an anticlinal structure and probably intruded the Birnin Gwari Schist Belt. The 2D magnetic forward modeling across the suspected BIF revealed an overburden thickness <300 m and a contrasting higher susceptibility of 0.009 (cgs unit) than the modelled neighbouring blocks. Estimation of the iron ore reserve was done using Hammer's mass model equation. The iron ore reserve was estimated to be ~8.97 x 10^8.The study therefore concluded that the banded iron mineralization in Birnin Gwari exists, cuts across Sofo Birnin Gwari, Malam Mudi and Kwadaga communities in an approximately N-S direction and has an estimate of ~89.7 million metric tons in reserve.

Keywords: Aeromagnetic data, Iron Ore mineralization, Filtering, Structural and Depth Analysis, Modelling

[1] Department of Geology, University of Benin, Benin City, Nigeria.
[2] Department of Geology, Faculty of Science, Obafemi Awolowo University, Ile-Ife, Osun State, Nigeria.
[3] Department of Geology, Faculty of Science, Obafemi Awolowo University, Ile-Ife, Osun State, Nigeria.
[4] Department of Geology, University of Benin, Benin City, Nigeria.

Introduction

Banded iron beds are important commercial sources of iron ore. In Nigeria, two broad types of iron ore depositshave been identified: Banded Iron Formation (BIF), which occurs in folded bands and lenses associated with the Precambrian meta-sedimentary schist belts, and Cretaceous sedimentary (oolitic) deposits (Adekoya, 1988). BIFs are chemical sedimentary rocks characterized by alternating layers of iron–rich minerals and chert (James, 1954), andthey are parts of relevant raw material used for steel production in Nigeria (Dada, 1988). In recent time, incessant exploitation of the Ajaokuta iron ore, which is the major iron ore mine in Nigeria, shows a high probability ofit getting close to depletion in few years' time. Also, the Agbaja and Enugu Sedimentary iron stone, which are reasonably large, are known to be of low quality (Adekoya, 1988). These have prompted the need for exploringmoreand better qualities of iron ore mineral in order to meet industrial demands.

Various geological and geophysical investigations have been carried out in Nigeria in search of iron deposits and results have shown the existence of iron ore deposits in different parts of the country (James 1954; Hazell, 1955; Jones, 1955; Adeleye and Dessauvagie, 1972; Stanton, 1972; Adekoya, 1988; Amigun*et al.*, 2012; Bolarinwa, 2018). According to Adekoya (1988) the iron formation in the northwestern Nigeria is classified into three facies: the oxide facies, silicate facies and sulphidefacies. The oxide facies commonly occurs as bandsof fine-grained quartz-hematite-magnetite or flaggy rocks with alternation of silica-rich and iron stone; the silicate facies are usually interbanded with the oxides facies and they occur as quartz-garnet-grunerite assemblage; while the sulphide facies is usually represented as the pyrite-bearing phyllites. In Birnin Gwari(northwesternNigeria), iron-formations of crystalline iron deposit werereported by Adekoya(1988). These deposits, which are oxide facies iron-formation,are fine grained and occur in narrow lenses or bands interbanded with mica schist (IPCO,1965; Adekoya, 1988). However, no geophysical evidence of this deposit has been reported.Therefore, the Birnin Gwari region of northwestern Nigeria has beenchosen in this study for detailed aeromagnetic investigation. This study aims to provide the geophysical evidence of the iron deposition, analyse the structural settings and estimate the tonnage of iron ore reserve in the area.

Magnetic method is used for detecting variation in geomagnetic field caused by changes in magnetic susceptibility of subsurface rocks. This method is used extensively in search formetalliferous mineral deposits, and this can be accomplished rapidly and economically using airborne methods.Airborne magnetic (aeromagnetic)method is an essential tool in delineating the regional geology (lithology and structure) of buried basement terrains. Theapplication of mathematical expressions on aeromagnetic data helps in delineating some geologicstructures and mineral deposits (Adepelumi & Falade, 2017).

Geology of the Study Area

The study area falls within the basement complex of Northwestern Nigeria bordering three states: Kaduna (SE), Zamfara (NW), and Katsina (NE). This region, which is situated between latitudes 11° 00' 00'' N to 11° 30' 00'' N and longitudes 6° 0' 00'' E to 6° 30' 00'' E, fall around the metasediments of both the Zungeru-Birnin Gwari and Kushaka schist formations in the Kusheriki

Schist Belt, NW, Nigeria. The area falls within the 1:200,000 standard topographic map of Kwiambana (sheet 100) N.W. of Nigeria and it is approximately 55 km. Detailed mapping was carried out by Truswell and Cope (1963) and extended southwards to the Zungeru area by Ajibade (1980). Four formations were recognized for the Kusheriki Schist Group, namely:

1. The Birnin Gwari Schist Formation,
2. The Zungeru Granulite Formation,
3. The Kushaka Schist Formation, and
4. The Kusheriki Psammite Formation at the base of the succession.

Zungeru-Birnin Gwari Schist Formation: the Birnin Gwari schist Fm and the underlying quartzo-feldspathic rock of the Zungeru Fm together form a single structural unit, named the Zungeru-Birnin Gwari Schist Belt which is Pan African in age. This forms a simple N-S syncline, 150km long, with the northern part displaced dextrally by a NE-SW transcurrent fault (Truswell and Cope, 1963). *The Zungeru member* outcrops on both flanks of the schist belt. It is largely made up of fine-grained quartzo-feldspathic rocks which are interbedded with amphibolites and some quartzites. Detailed geology about the study area is contained in texts by (Kogbe, 1989; Obaje, 2009).

Figure 1: Geological Map of the Study Area

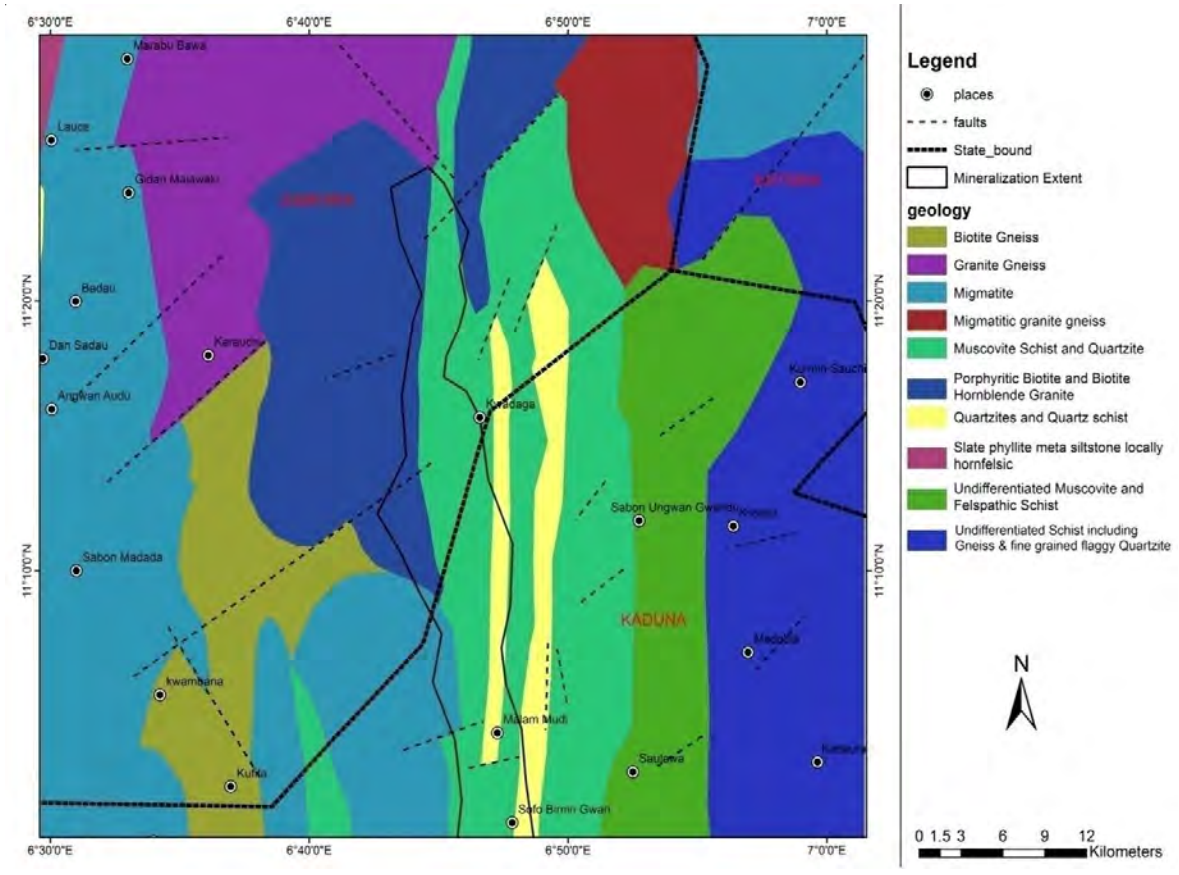

Source: Adopted from NGSA 2006

Methodology

Aeromagnetic data of part of northwestern Nigeria was acquired from the Nigeria Geological Survey Agency (NGSA). The aeromagnetic survey was carried out between 2005 and 2009 by Fugro Airborne Surveys for the NGSA. The data covered an area of about 3,025 km^2 (latitudes 11° 0' 00''N " 11° 30' 00''N and longitudes 6° 30' 00''E " 7° 0' 00''E), and it was recorded at an interval of 0.1 s (~7.5 m). The aircraft used for the data acquisition was flown at flight line spacing of 500 m, terrain clearance of 80 m, tie line (NE–SW direction) spacing of 2 km and in NW-SE direction. All essential data corrections, which include IGRF removal, were done by Fugro Airborne Surveys.

All data processingwas carried out using Geosoft package software (Oasis Montaj™, version 6.4.2.). The aeromagnetic data was gridded at 100 m grid interval, using minimum curvature technique, to produce the Total Magnetic intensity (TMI) anomaly map (Figure 2). One-fifth of the survey flight line spacing was used for the grid interval in order to avoid short wavelength error which may appear as lines perpendicular to the survey flight line (Anudu *et al.,* 2014; Adepelumi and Falade, 2017). Afterwards, the map was reduced to the equator (Figure 3), using magnetic inclination (–0.265°) and declination (–1.741°) of the centre point of the study area. Unwanted deep-seated signals, which include the regional fields, were removed by upward continuing the Reduction-to-Equator (RTE) map to a height of 10 km, and the resulted map was subtracted from the RTE map to obtain the residual map. After this, near surface features were removed by upward continuation of the residual map to a height of 100 m. The obtained Filtered Residual Magnetic Anomaly (FRMA) map is shown in Figure 4. Subsequently, various filtering and transformation such as Horizontal Gradient Magnitude (HGM), First Vertical Derivative (FVD), pseudogravity, apparent susceptibility and depth analysis, using Source Parameter Imaging (SPI) technique, were carried out on the filtered residual map to obtain their corresponding maps (Figures 5a and b, 8, 9 and 10). The results obtained from FVD and HGM were exported to ArcGIS software to map out geologic lineaments. The inferred lineament map is shown in Figure 6. Azimuthal directions of the geologic linear features were calculated and fed into Georose software to obtain summary of azimuthal distribution of the lineaments. Figure 7 shows the azimuthal frequency of the inferred geologic lineaments. For estimation and detection of suspected BIF formation, the anomalous zones on the apparent susceptibility and pseudogravity mapswere studied, and areas with relatively high density value and high magnetic susceptibility, which are typical of BIF, were correlated on both maps to depict the BIF. A 2D magnetic forward modelling (Fig 11b), was carried out across the suspected BIF using GYM-SYS™ module of Oasis Montaj in order to ascertain the magnetic susceptibility, location and overburden thickness of the suspected BIF. Finally, tonnage estimation of the BIF deposit was carried out using Hammer's mass block model. The suspected BIF region on the pseudogravity map was divided into three blocks and each block's tonnage was computed and summed together to obtain the tonnage of iron ore reserve across the study area.

Reduction to the equator (RTE) has an amplitude component (the sin (I) term) and a phase component (the Icos (I) cos (D-δ) component). When reducing to the equator from low latitudes, North-South features can blow-up due to the numerical error (from the term of 0/0)

in amplitude correction (the sin (*I*) component) that is applied when (*D*-δ) is δ/2 (i.e. a magnetic east-west wave number). This problem can be reduced or eliminated at the expense of slightly under-correcting the amplitudes of near North-South features expressed in the Geosoft Oasis Montaj Software as:

$$L(\theta)=\frac{[\sin(I)-i.\cos(I)\cos(D-\theta)]^2\times(-\cos^2)(D-\theta)}{[\sin^2(Ia)+\cos^2(Ia).\cos^2(D-\theta)]\times[\sin^2(I)+\cos^2(I).\cos^2(D-\theta)]'}$$

$$\text{if } (|Ia|<|I|), Ia=I \qquad ...(1)$$

where: *I* geomagnetic inclination, Ia inclination for amplitude correction (never less I), *D* geomagnetic declination.

HGM of potential field anomalies is steepest approximately over edges of tabular sources (Dobrin and Savit 1988). The maxima of horizontal gradient are located at the edges of the tabular body and this can assist when inspecting for magnetization contrasts. The magnitude of the horizontal gradient of the RTP, RTE, or pseudo-gravity transformation of a gridded magnetic field data is given by:

$$HGM(x,y)=\sqrt{\left(\frac{\partial M^2}{\partial x}\right)^2+\left(\frac{\partial M^2}{\partial y}\right)} \qquad ...(2)$$

For gridded data, $\frac{\partial M}{\partial x}$ and $\frac{\partial M}{\partial y}$ are the field gradients in the x (East) and y (North) directions, respectively and *M* is the reduced to the pole magnetic field.

The first vertical derivative (FVD) is useful in enhancing shallow sources, suppressing deeper ones, to emphasize the effects of geological contacts, critical for the structural framework and giving a better resolution of closely-spaced sources. The equation by Reeves (2005) of the wave number domain filter to produce nth derivative is expressed as:

$$F(\omega)=\omega n \qquad ...(3)$$

The data was gridded at 100m grid spacing and subjected to regional/residual separation to isolate short-wavelength signal which is more suitable for high-resolution mapping of shallow magnetic boundaries. The enhancement of magnetic anomalies associated with faults and other structural discontinuities were achieved by the application of FVD to the filtered residual map in Figure 5 (Dobrin and Savit, 1988; Telford et al., 1990). The reprocessed aeromagnetic data set is significantly enhanced in high frequencies and is much better suited to detailed regional shallow mapping and analysis of basement magnetic boundaries (Feumoe *et al*.,2012).

The source parameter imaging (SPI) technique is one of the methods used for in depth to magnetic basement. This method sources its parameters from gridded data and uses an extension of complex analytical signal to estimate the magnetic source depth. The technique (sometimes referred to as the local wave number method) is a profile or grid based method that estimates the magnetic source depth, dip, and susceptibility contrast of some source geometries (Thurston and Smith 1997; Thurston et al. 1999, 2002; Nwosu 2014).The SPI method (Thurston and Smith 1997) estimates the depth from the local wave number of the analytic signal. The analytic signal A1 (x, z) is defined by Nabighian (1972) as:

$$A_1(x,z)=\frac{\partial M(x,z)}{\partial x}-j\frac{\partial M(x,z)}{\partial z} \qquad ...(4)$$

Nabighian (1972) shows that the horizontal and vertical derivatives comprising the real and imaginary parts of the 2D analytic signal are related as follows:

$$\frac{\partial M(x,z)}{\partial x}\Leftrightarrow-\frac{\partial M(x,z)}{\partial z} \qquad ...(5)$$

where !denotes a Hilbert transform pair. The local wavenumber k1 is defined by Thurston and Smith (1997) to be:

$$K_1 = \frac{\partial}{\partial x}\tan^{-1}\left[\frac{\partial M}{\partial z}\Big/\frac{\partial M}{\partial x}\right] \quad ...(6)$$

We use the concept of an analytic signal comprising second-order derivatives of the total field, in a manner similar to that used by Hsu *et al.* (1996). The analytic signal defined by Nabighian (1972) uses the Hilbert transform pair in (2). The Hilbert transform and the vertical-derivative operators are linear, so the vertical derivative of (2) will give the Hilbert transform pair:

$$\frac{\partial^2 M}{\partial z \partial x} \Leftrightarrow -\frac{\partial^2 M(x,z)}{\partial^2 z} \quad ...(7)$$

This enables us to define an analytic signal based on second-order derivatives, $A_2(x, z)$, where:

$$A_1(x,z) = \frac{\partial^2 M(x,z)}{\partial z \partial x} - j\frac{\partial^2 M(x,z)}{\partial^2 z} \quad ...(8)$$

This gives rise to a second-order local wavenumber k_2, where:

$$K_2 = \frac{\partial}{\partial x}\tan^{-1}\left[\frac{\partial^2 M}{\partial^2 z}\Big/\frac{\partial^2 M}{\partial z \partial x}\right] \quad ...(9)$$

The first and second-order local wavenumbers are used o determine the most appropriate model and a depth estimate independent of any assumptions about a model.

The pseudo-gravity transform (Baranov, 1957) is applied to the magnetic data. By using the pseudo gravity transform, the apex of the magnetic anomalies is shifted over the source body and the distortion due to the earth's magnetic field can easily be removed, (Feumoe et al., 2012). A pseudo-gravity transformation is useful in interpreting magnetic anomalies, not because a mass distribution actually corresponds to the magnetic distribution beneath the magnetic survey, but because gravity anomalies are in some ways more instructive and easier to interpret and quantify than magnetic anomalies (Blakely, 1995). The pseudo-gravity transformation as expressed from Poisson's relation:

$$v(p) = -MV_p \iiint \frac{1}{d} dv \quad ...(10)$$

where *p* is the observation point, d the distance from p. The gravitational potential is:

$$U(p) = G_p \iiint \frac{1}{d} dv \quad ...(11)$$

where *G* is the gravitational constant and r the density. Combining the two,

$$V(p) = -\frac{1}{G_p} MV_p U = -\frac{1}{G_\rho} Mg_M \quad ...(12)$$

g_M the component of gravity in the direction of magnetization: it is Poisson's relation. In fact, it is not necessary for gravity and magnetization to be constant.

Results and Discussion

Qualitative Interpretation

Qualitative interpretation is the cornerstone of magnetic interpretation. It involves visual recognition of discrete anomalous zones such as intrusions, faults, structural grain, disruptive cross-cutting features and unifying tectonic features. The study area is characterized by magnetic intensity values that range from –67.1 to 85.4 nT (Figure 2). High magnetic intensities are found across the study area, but they are more dominant in the northern, eastern and WSW part of the study area. These anomalies are long wavelength anomalies whose sources are from deep-seated basement rocks. The map also

shows a dominating short wavelength tabular anomalies trending mostly in E-W direction. The study area is characterized by magnetic relief of 153 nT, and this can be attributed to the difference in magnetic properties of both basement and intra sedimentary rocks.

Reduction to Equator and Computation of Residual

The comparison of anomalies observed in both TMI and RTE maps (Figures 2 and 3) show an insignificant difference. This is as a result of low magnetic inclination (–0.265°), which can be attributed to the closeness of the study area to the magnetic equator, used for the RTE filtering. The magnetic intensity of the maps reduced from 85.4 to 63.7 nT, while the low intensity areas increased from -67.1 to -63.4nT.

Figure 4 shows the FRMA map. In low latitude regions (such as the study area), areas with negative magnetic intensity correspond to high susceptibility, while positive magnetic intensity areas corresponds to low susceptibility. The NE and SW regions (Figure 4) show deep seated anomaly patterns that are characterized with high susceptibilities. The southern region down to the central region of the map shows intercalations of magnetic highs and lows. A visual study of these anomaly patterns revealed that these paired anomalies may be due to the intrusions within the basement rock. Long wavelength anomalies of low magnetic susceptibilities are prominent at northern, eastern and WSW part of the study area. The magnetic field intensity values, as shown on the legend of the map, range from - 69

Figure 2: Total Magnetic Field Intensity (TMI) Anomaly Map of the Study Area

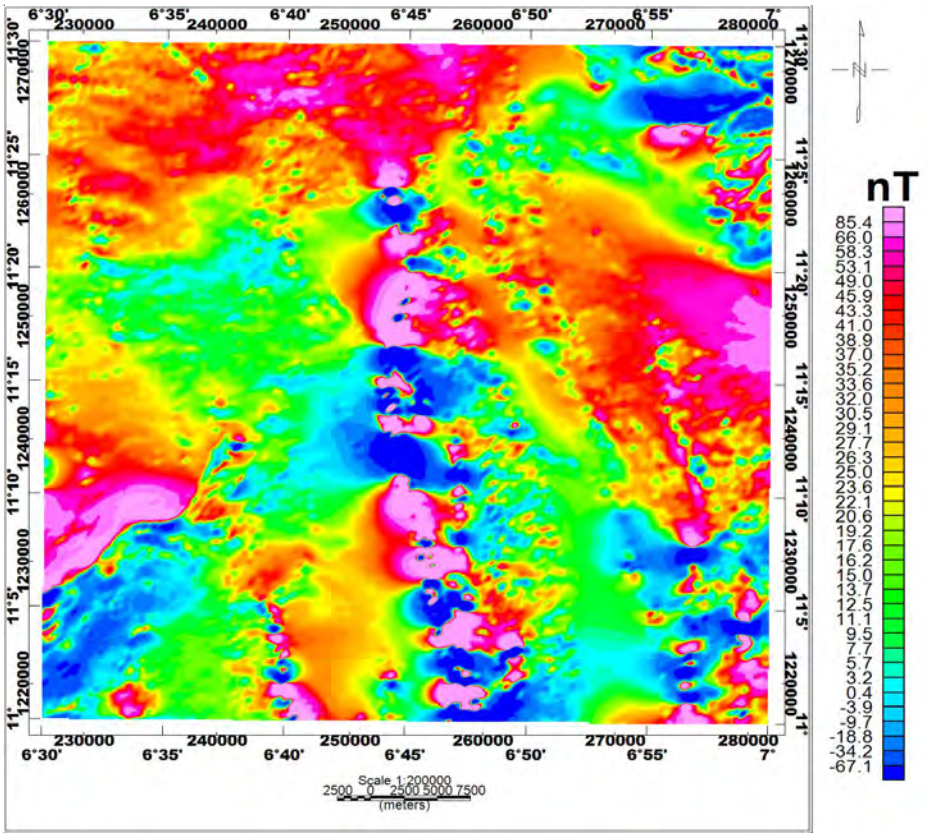

Figure 3: Reduction to the Equator (RTE) Map of the TMI Map

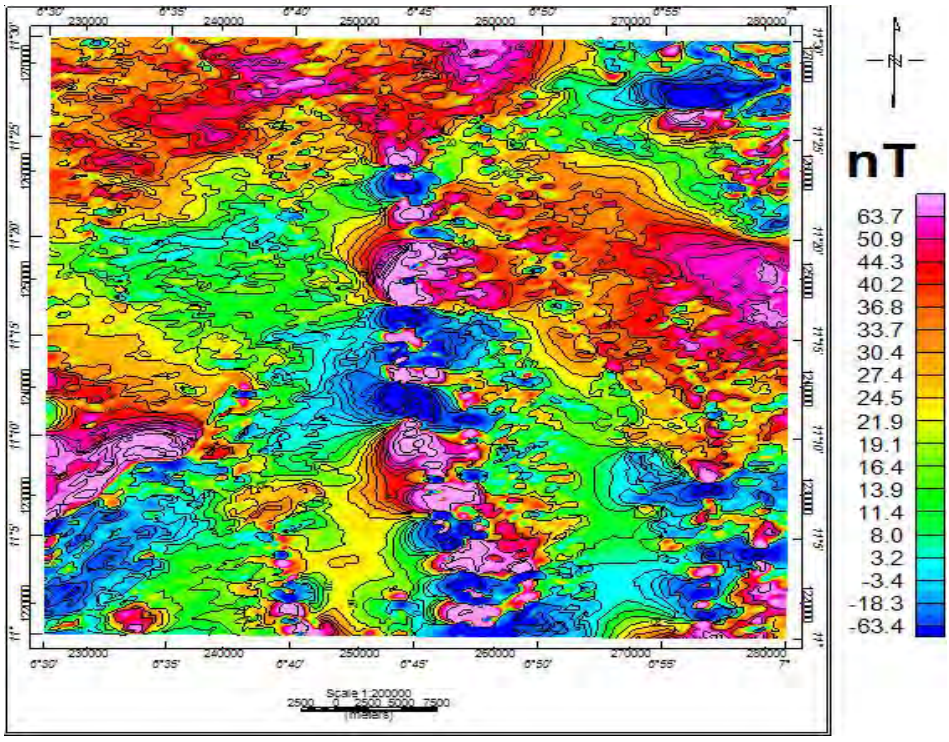

Figure 4: Filtered Residual Map

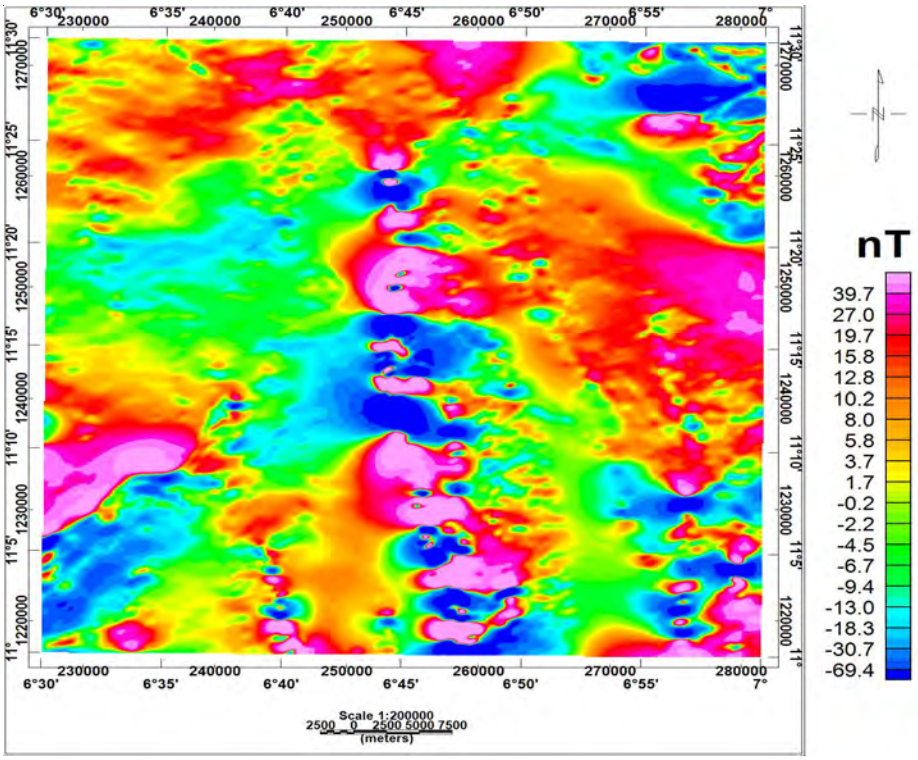

to 40 nT. These disparities in magnetic intensities could be attributed to variations in magnetic minerals of the basement rocks, residual soils and discrepancies in the overburden thicknesses of these basement rocks.

Lineaments Analysis

First Vertical Derivative (FVD) and Horizontal Gradient Magnitude (HGM) Maps

In this study, two derivatives, FVD and HGM, were utilized for mapping linear geologic features. Figures 5a and 5b show the maps of these derivatives. Overlain on each map respectively are the locations of peaks of HGM and near minima of FVD, showing the edges of geological structures. More edges are revealed on the FVD map than HGM map, because FVD technique amplifies more near surface features (including noises). However, the HGM map reveals more continuous edges of geological features.

On these maps (Fig 5a and b), the edges of the structures were revealed to trend mostly in ENE-WSW direction. The southern and the

Figure 5(a): FVD Zeros Location Superimposed Upon FVD Map

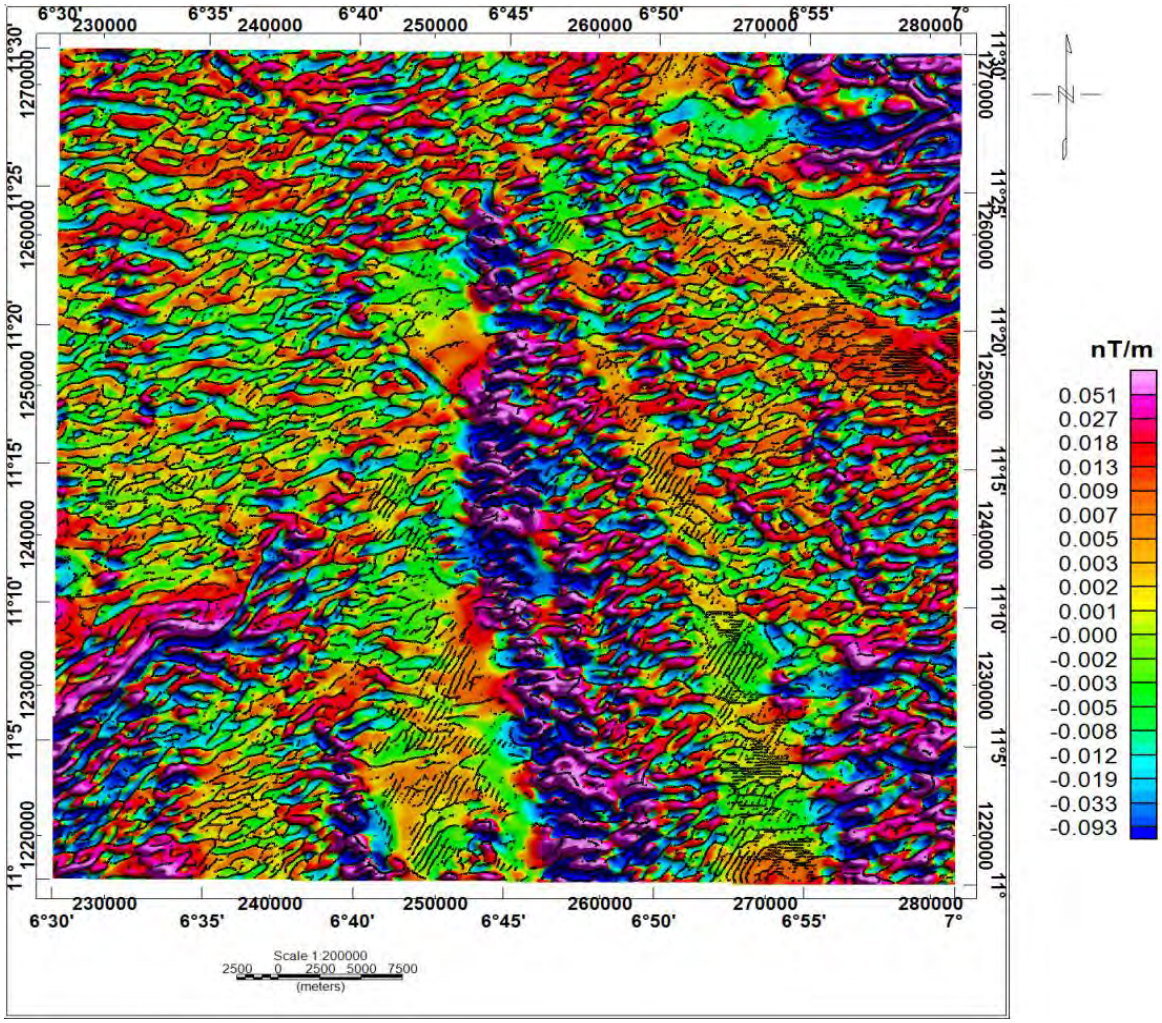

Figure 5(b): HGM Maxima Overlain Upon HGM Map

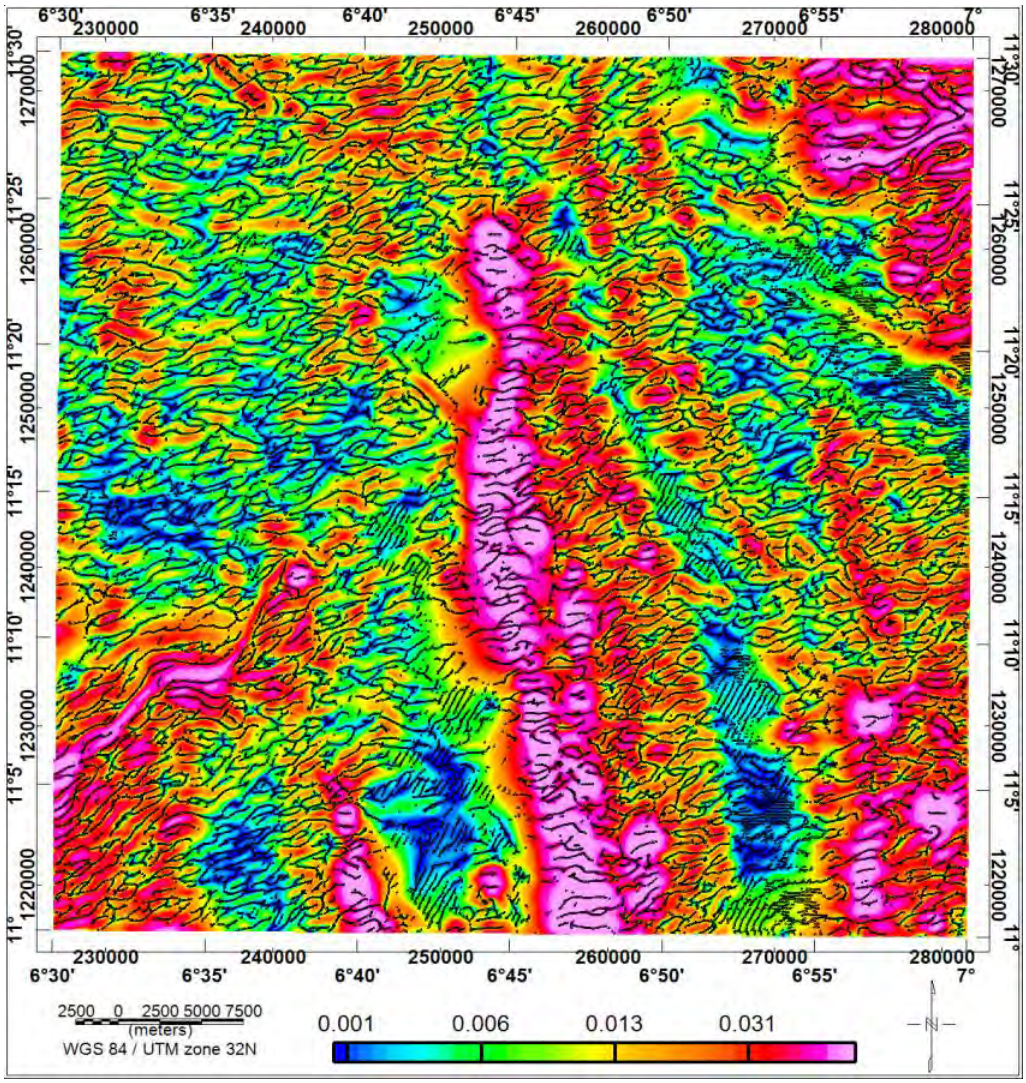

central regions are predominated with contacts trending in E-W direction. Other edges trending in NE-SW, WNW-ESE, NW-SE and NNW-SSE directions were also observed on these maps.

Inferred Lineament Map

The inferred lineament map of the study area is shown in Figure 6, while the azimuth-frequency (Rose) diagram of this inferred lineament map is shown in Figure 7. The rose diagram depicts that the inferred lineament map is predominated with geologic lineaments trending in the ENE-WSW direction; other geologic linear features observed in the study area trend in NE-SW, WNW-ESE, NW-SE and NNW-SSE directions. Most of these structural trends are in conformity with the geologic setting of the study area. The closely spaced sub-parallel linear orientation structures were observed mostly in the central portion of the inferred lineament map. The variation in the strike directions of these geologic linear features suggest that the area was subjected to more than a single tectonic event.

Figure 6: Inferred Lineament Map of the Study Area

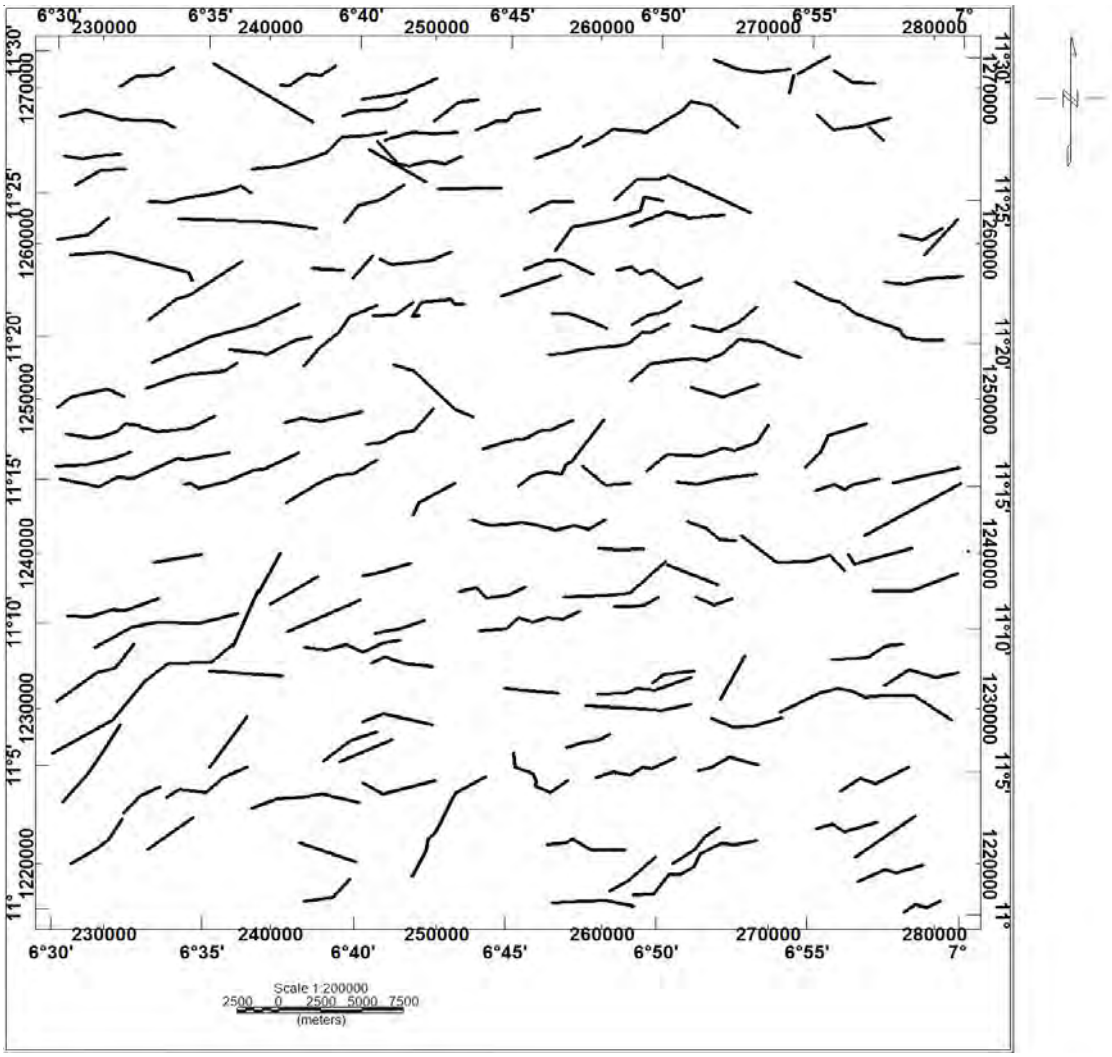

Figure 7: Azimuth-Frequency (Rose) Diagram of the Inferred Lineament Map

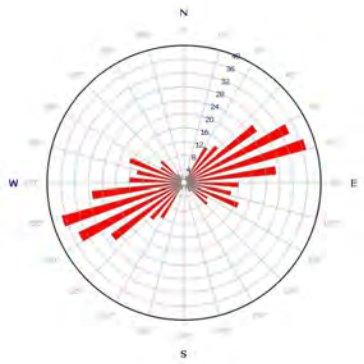

Depth Analysis Using SPI Technique

Figure 8 shows the depth estimates obtained from the SPI technique. From Figure 8, the overburden thicknesses of the area range between 119 and 1304 m. About 70% of the study area contains sources that are relatively shallow (< 300 m). The ENE portion and the SSE up to the central part, labelled as A and B, have the highest overburden thickness. However, deeper magnetic sources are scattered around the study area. The area

Figure 8: Source Parameter Image (SPI) Depth Map

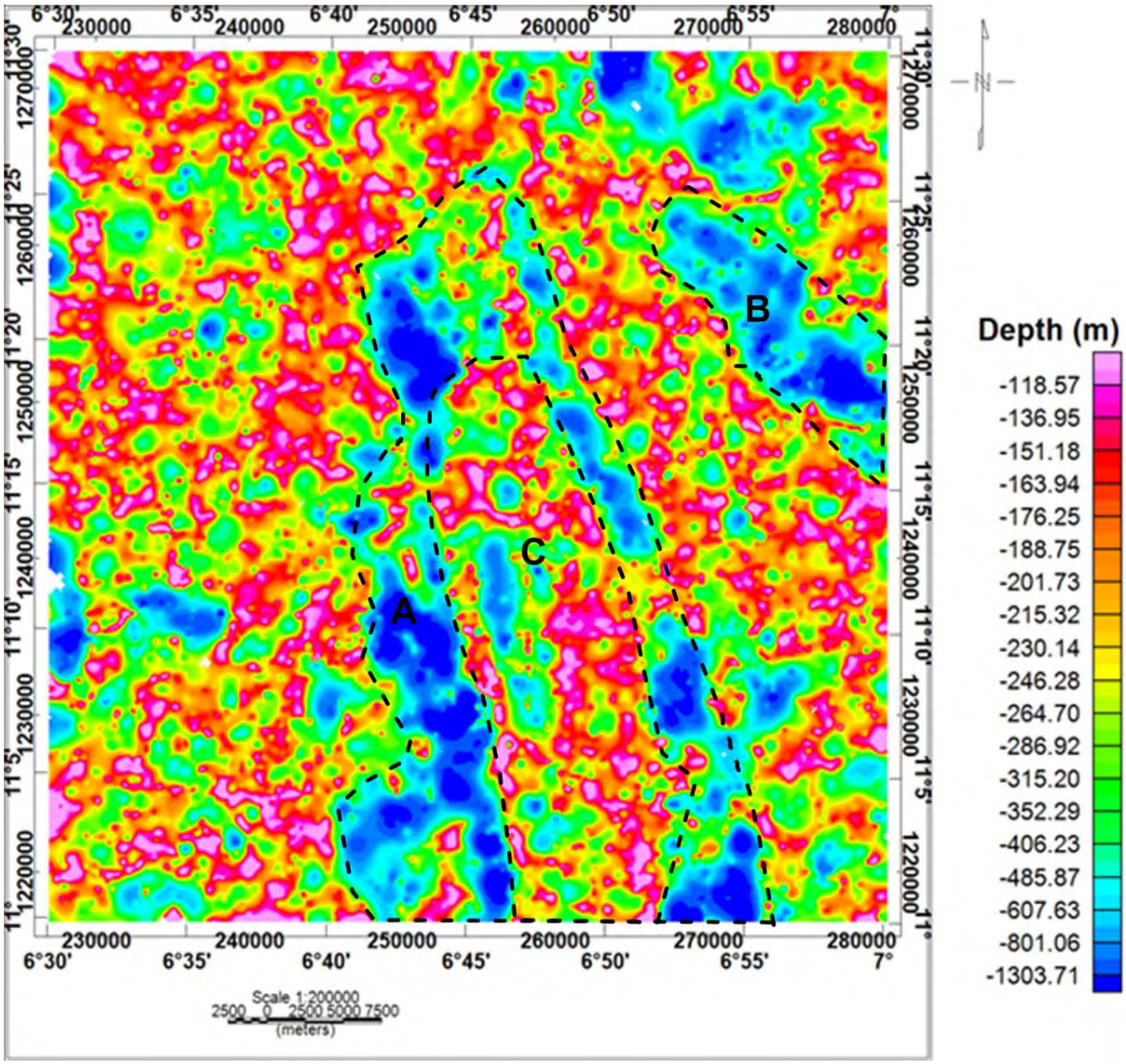

labelled 'C' whose sources are relatively shallow, compared to surrounding 'A', could possibly be an intrusion in the region demarcated as A.

Apparent Susceptibilty and Pseudogravity

The apparent susceptibility filter works on the assumption that: the IGRF has been removed, there is no remanent magnetization and magnetic response is caused by a collection of vertical prisms of infinite depth and strike extent (Geosoft, 2009). In this study, the apparent susceptibility map helped in defining the magnetization domains within the study area. The apparent susceptibility map of the study area is shown in Figure 9. The north-south alignment observed on the map is as a result of reduction to the pole filtering

incorporated in the susceptibility filter. The apparent susceptibility value, in emu unit, of the study area is classified into very high (>0.00060), high (0.000008 " 0.000463), low (-0.000342 " 0.000085) and very low (< -0.000342) susceptibility. Low susceptibility values dominate the study area with few intercalations of highs. However, the SSE part down to the central part is dominated with relatively very high susceptibility value. The very high value recorded in this region is possibly due to magnetic responses from the BIF. Within the highs, the low susceptibilities observed within the highs are probably responses from pelites interbedded within the BIF. Also, the northeastern region also shows a very high susceptibility value; this could probably be the magnetic response from the basement rock.

Pseudogravity transformation is useful in interpreting magnetic anomalies because gravity anomalies are in some ways more instructive and easier to interpret and quantify than magnetic anomalies (Blakely, 1995). Also, gravity data helps in determining mass distribution across an area and which is invariably used for estimating the tonnage of an iron ore body (Hammer, 1945; Parasnis, 1986). Figure 10 shows the pseudogravity map of the study area. The suspected BIF shows relatively high density value of about 0.068 mgal, while the eastern and western regions are characterized by low density value.

Comparing the apparent susceptibility map (Figure 9) with the pseudogravity map (Figure 10), it is readily apparent that the main pseudo-gravity peak correlates with the peak of the apparent

Figure 9: Apparent Susceptibility Map of the Study Area

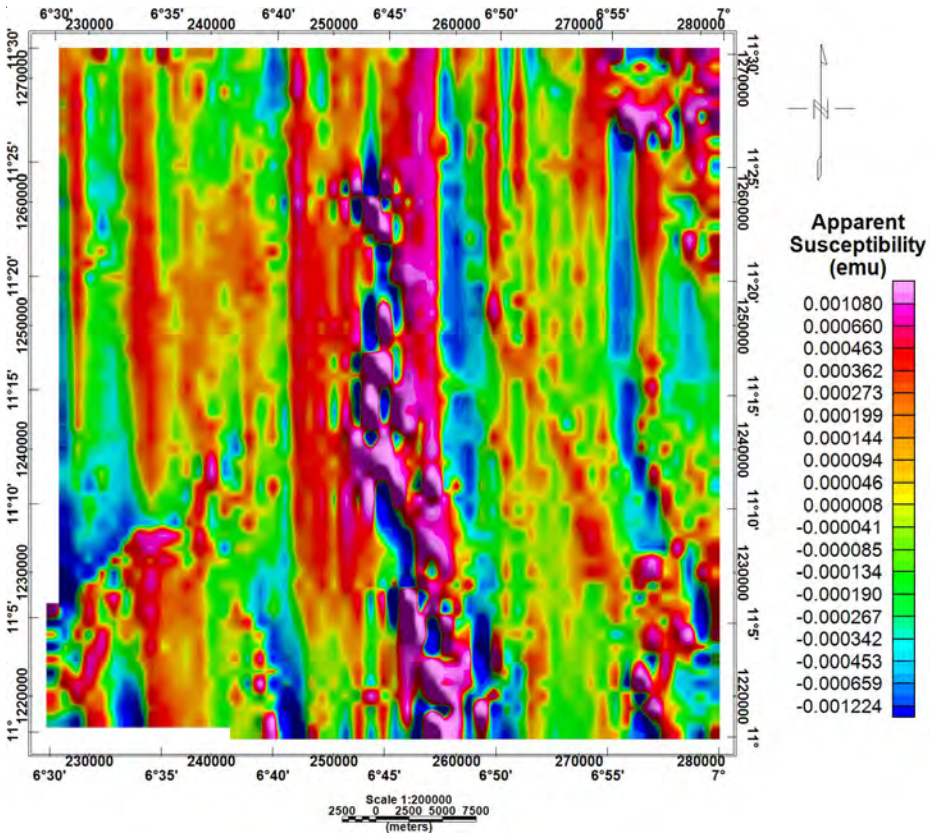

Figure 10: Pseudogravity Map and Selected Blocks A, B, C for Reserve Estimation

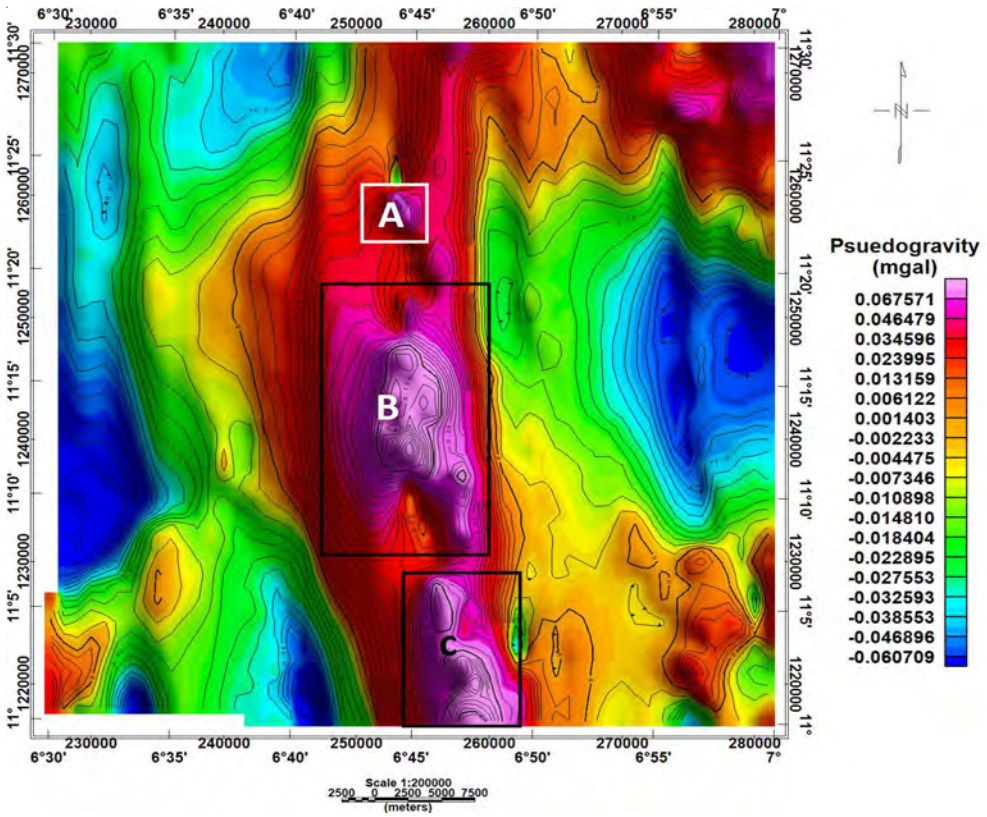

susceptibility map. The maps suggest that the density features responsible for the gravity maxima are also magnetic. Thus, these observed high anomalies are typical of a BIF.

2D Forward Mpdeling

In order to accurately measure the magnetic susceptibility and provide the 2D image along the suspected BIF, a 2D magnetic modelling of profile A-A' (Figure 11a), taken across the suspected BIF, was carried out. The profile was taken in NE-SW direction, and the SPI depth was used as constraint in order to reduce the ambiguity in magnetic modelling. The 2D magnetic model is presented in Figure 11b; Figure 11b revealed the depth to the magnetic basement to be in the range of 60 to 920 m. 14 basement blocks were modelled along the profile with susceptibility value varying between ~0.001 to ~0.009 (cgs unit). The contacts between these basement blocks are shown to be near vertical. Block 6 shows the highest susceptibility value compared to other blocks. This block, block 6, is also characterized with high apparent susceptibility and density value on apparent susceptibility and pseudogravity maps (Figures 9 and 10) respectively.

Therefore, the 2D modelling revealed that the basement rock along the BIF exists at a depth of about 240 m and it is characterized with susceptibility value of ~0.009 (cgs unit).

Possible Iron Ore Reserve Estimation

Hammer's mass estimation theorem, modified in Kearey *et al.* (2002), was used for estimating the tonnage of iron ore reserve in this study area.

Figure 11(a): Profile A-A' Selected Across the Suspected BIF

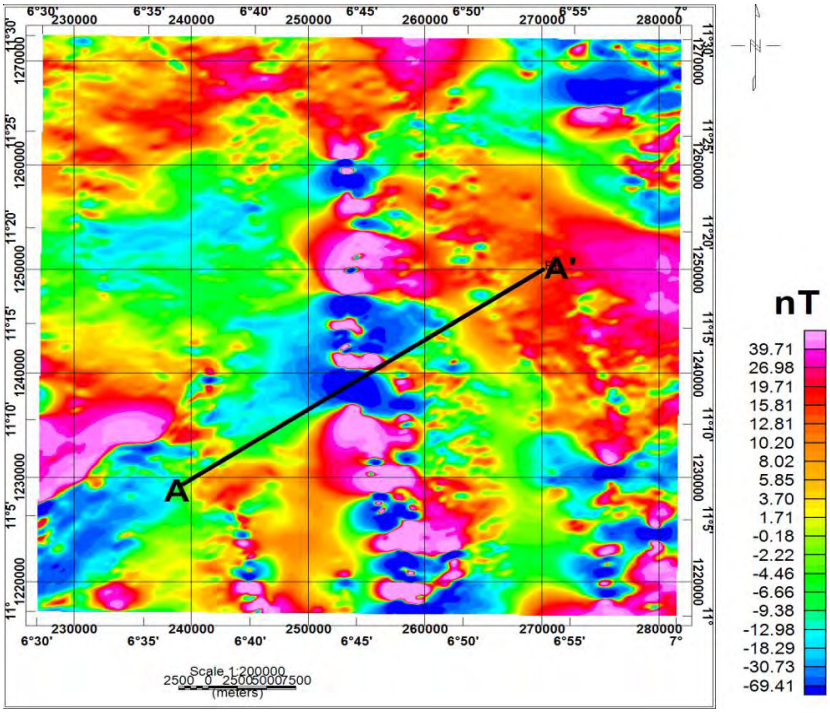

Figure 11(b): 2D Magnetic Forward Model Across the Suspected BIF

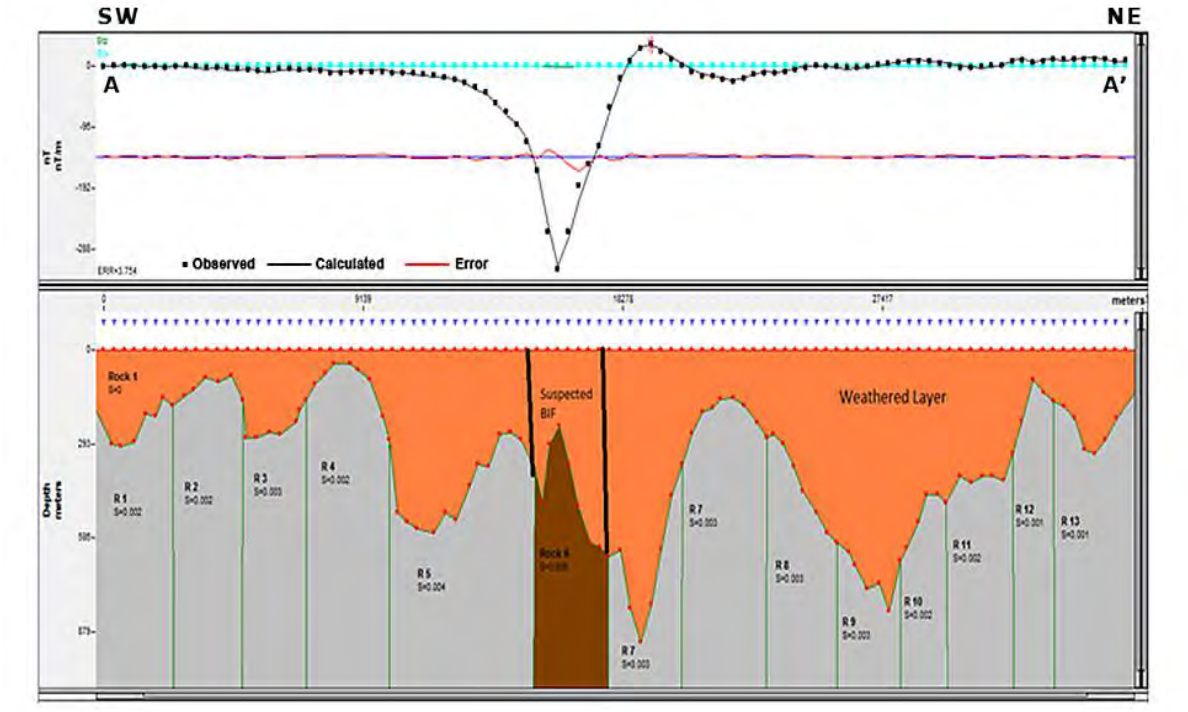

This was carried out with the aim of determining the possibility of developing the area into a mine. According to Parasnis (1986), mass estimation can be determined from an observed gravity data using Hammer's mass estimation theorem. Excess mass according to Kearey *et al.* (2002) is the difference in mass between the body and the country rock. The excess mass across the suspected BIF was calculated using the pseudogravity map (Figure 10). Three different density highs are clearly shown in an approximately north-south trend (Figure 10). These anomalous (mineralized) zones were divided into three blocks A, B and C as shown in Figure 10. The areas of these blocks, in square kilometres, were calculated using the block model of Geosoft Oasis Montaj software. Thereafter, the excess mass was estimated using the Hammer's equation below.

$$M_e = \frac{1}{2\pi G}\sum_{i=1}^{n} \Delta g_i \Delta a_i$$

Where Δ_g and Δ_a are the mean residual anomaly and area of each block, while G is the gravitational constant.

The following excess masses were obtained for A, B, C.

A = ~4.00 x 10^7 metric tons

B = ~4.2 x 10^8 metric tons

C = ~1.36 x 10^8 metric tons

According the Adekoya (1988), Turner (1983) and as also shown on the geologic map (Fig. 1), the suspected BIF is hosted by schist. The actual mass of these bodies is:

$$M = \frac{\rho_1 M_E}{(\rho_1 - \rho_2)}$$

ρ_1 = *density of the anomalous body*

ρ_2 = *density of the country rock = schist*

M = ~8.97 x 10^8 metric tons.

Figure 13: Map Showing the Inferred Areal Extent of Iron-ore Mineralization in the Study Area

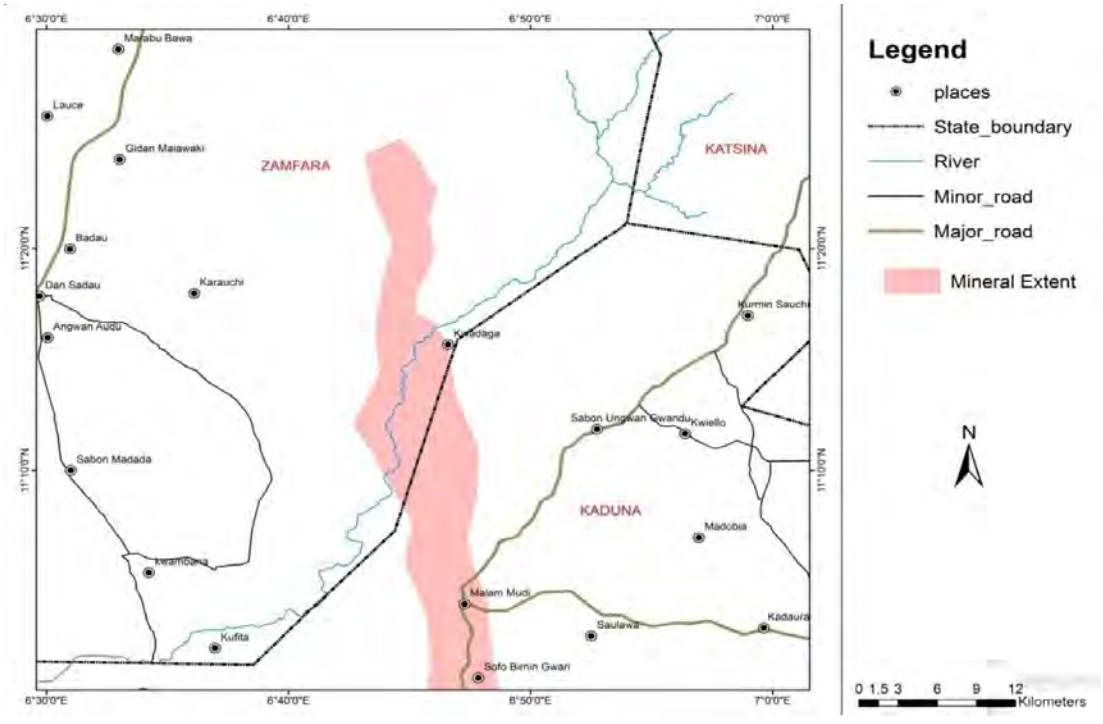

Therefore the estimated iron ore reserve in Birnin Gwari is ~8.97 x 10^8 metric tons.

Discussion

The BIF in Birnin Gwari, according to Adekoya (1988), is interbanded with garnet quartz-mica schist, orthoquartzites and carbonaceous schist. These interbanded rocks are probably shown on the TMI anomaly map (Figure 2), along the suspected BIF, as intercalations of magnetic highs and lows. The closely spaced linear sub-parallel orientation of contours at central portion of the TMI anomaly map (Figure 2), suggests the possibility of faults and folds passing through these areas. Grant (1978) and Adekoya (1988) reported that the Birnin Gwari schist formation is intensely deformed into multiple minor folds with parallel folds. This suggests that the area has been subjected to tectonic activities. From the inferred lineament map (Figure 6), various geologic linear features % trending in ENE-WSW, NE-SW, WNW-ESE, NW-SE and NNW-SSE directions, of which the ENE-WSW and NE-SW geological features predominates % confirmed that Birnin Gwari region has been subjected to various tectonic activities. The NE-SW structures were believed to be associated with the PAN African Crustal Consolidation event, the E-W structures were said to be pre-Pan African ((Obiora, 2009; Mullan, 1978), while the NW-SE were identified with Kibaran orogeny (Kogbe, 1989). The emplacement of some granitic rocks (charnockites and Older Granites) into the pre-existing basement complex rocks (migmatite-gneiss complex and younger metasediments) occurred during the Pan-African event and this, however, resulted into the reduction of metasediments to infolded synformal remnants (Russ, 1957; Grant, 1969; Adekoya, 1988). While in the Kibaran era, the basement rocks and its overlaying sediments, containing iron-formation, were subjected to deformation and metamorphism (Ogezi, 1977; Adekoya, 1988). Therefore, this Precambrian metamorphic iron bearing rocks could be traced to the Kibaran and pre-Kibaran era.

The 2D forward model (Figure 11b) shows relatively high susceptibility value across the suspected BIF. Also, the apparent susceptibility and pseudogravity maps, (Figures 9 and 10) show anomalous highs, typical of magnetite rich and highly dense basement rock, aligning in the N-S direction. On the SPI map (Fig. 7), the location of the BIF is shown as suspected basement intrusion. These results agreed with the geological report of Turner (1983) and Adekoya (1988) that the BIF is enclosed within the Birnin Gwari schist belt and conformable with the N-S strike direction of the schist belt. The results from the SPI, apparent susceptibility and pseudogravity maps, were used to deduce the areal extent of the iron ore mineralized zone (Figure 13). From Figure 13, the mineralization could be traced further south from Sofon Birnin-Gwari towards Malam-Mudi and cuts through the Koriga River and Kwadaga town in Zamfara State.

Finally, the tonnage estimate of iron ore reserve of the Birnin Gwari deposition was computed from the pseudogravity map using Hammer's excess mass equation. An estimate of 89.7 million metric tons of iron ore was computed for the study area.

Conclusion

The analysis of aeromagnetic data over Birnin Gwari region has revealed the presence of iron ore mineralization in the region. The results show that area has been subjected to various tectonic activities resulting into faulting and folding of

basement rocks. Various geologic linear features were observed in this region of which the ENE-WSW structural trend predominates. The 2D magnetic forward modelling across the suspected BIF, pseudogravity and apparent susceptibility maps confirmed the deposition of iron ore deposit and which exists at a depth lesser than 300 m. The comparison of suspected BIF with geological map shows that the BIF trend in the same direction (N-S direction) with the Birnin Gwari schist belt and it is enclosed within the schist belt. The tonnage and deposit size of the iron ore bodies were estimated using Hammer's mass equation modified by Kearey *et al.* (2002). From the estimation, the iron ore deposit in this area is ~89.7million tons in mass.

The study therefore concluded that the banded iron mineralization in Birnin Gwari exists and cuts across Sofo Birnin-Gwari, Malam-Mudi and Kwadaga communities in an approximately N-S direction, and the probable estimate of the iron ore reserve is ~89.7 million metric tons.

References

1. Adekoya J A (1988), "Precambrian Iron Formation of Northwestern Nigeria. Precambrian Geology of Nigeria", *Geological Survey of Nigeria*, pp. 195-210.
2. Adeleye D R and DessauvagieT F J (1972), "Stratigraphy of the Niger embayment near Bida, Nigeria", in *African Geology*, T F J Dessauvagie and A J Whiteman (Eds.), 1970, pp. 181-186, University of Ibadan.
3. Adepelumi A A and Falade A H (2017), "Combined high-resolution Aeromagnetic and Radiometric Mapping of Uranium Mineralization And Tectonic Settings in Northeastern, Nigeria. ActaGeophysica, Springer, ISSN 1895-6572.
4. Amigun J O, Afolabi O and Ako B D (2012), "Application of Airborne Magnetic Data to Mineral Exploration in the Okene Iron Ore Province of Nigeria", *International Research Journal of Geology and Mining*, Vol. 2, No. 6, pp. 132-140.
5. Anudu G K, Stephenson R A and Macdonald D M (2014), "Using High Resolution Aeromagnetic Data to Recognise and Map Intra Sedimentary Volcanic Rocks and Geological Structures Across the Cretaceous middle Benue Trough, Nigeria", *Elsevier J Afr Earth Sci.,* Vol. 99, pp. 625–636.
6. Baranov W (1957), "A New Method For Interpretation of Aeromagnetic Maps: Pseudo-Gravimetric Anomalies", *Geophysics.*, Vol. 22, pp. 359–383.
7. Blakely R J (1995), "Potential Theory in Gravity and Magnetic Applications", Cambridge University Press, pp. 331-355.
8. Bolarinwa A T (2018), "Petrography and Geochemistry of the Banded Iron Formation ofthe Gangfelum Area, Northeastern Nigeria", *Earth Science Research*, Vol. 7, No. 1, pp. 25-34.
9. Dada O (1988), "The 'Schist' Belt of the Nigerian Precambrian and its Potential for Raw Material Development for Steel Plants in Nigeria".
10. Dobrin M B and Savit C H (1988), *Introduction to Geophysical Prospecting*, 4th Edition, McGraw-Hill Book Co. Inc. New York. pp. 152-190, 498-578, 691-745.
11. Feumoe A N S, Ndougsa-Mbarga T, Manguelle-Dicoum E and Fairhead J D (2012), "Delineation of Tectonic Lineaments

Using Aeromagnetic Data For the South-East Cameroon Area*, GEOFIZIKA,* Vol. 29.

12. Geosoft Reference Manual (2009), Software for Earth Sciences Geosoft INC., Toronto, Canada.
13. Grant N K (1969): The Late Precambrian to early Paleozoic Pan-African Orogeny in Ghana, Togo, Dahomey and Nigeria. Geol. Soc. Amer. Bull., Vol. 80, pp. 45-56.
14. Grant N K (1978), "Structural Distinction Between a Metasedimentary Cover and an Underlying Basement in the 600-m.y. Old Pan-African Domain of Northwestern Nigeria, *West Africa. Geol. Soc. Amer. Bull.*, Vol. 89, pp. 50-58.
15. Hammer S (1945), "Estimating ORE Masses in Gravity Prospecting", *Geophysics*, Vol. 10, pp. 50–62.
16. Hsu S K and Sibuet J C (1996), "High Resolution Detection of Geologic Boundaries From Potential Field Anomalies: An Enhanced Analytic Signal Technique", *Geophysics,* Vol. 61, pp. 373-386.
17. IPCO (1965), "Mineral Deposits of Western Nigeria, Unpublished Report of Internationale PLannungs – und Consulting G M B H", Western Germany to the Western Nigeria Government.
18. James H L (1954), "Sedimentary Facies of Iron-formation", *Econ.Geology*., Vol. 49, pp. 235-293.
19. Jones H A (1955), "The Oolitic Ironstone of the Agbaja Plateau, Kabba Province", *Rec. Teol. Surv. Nigeria*, pp 20-35.
20. Kearey P, Brooks M and Hill I (2002), "An Introduction to Geophysical Exploration. Blackwell Science Ltd.", 3rd Edition.
21. Kogbe C A (1989), "Geology of Nigeria", 2nd Edition, Rockview Nigeria Ltd.
22. Mullan H S (1978): Structural Distinction Between a Metasedimentary Cover and an Underlying Basement in the 600my Old Pan-African Domain of Northwestern Nigeria, West Africa", *Discussion. Geol. Soc. Am. Bull*., Vol. 89, pp. 983-984.
23. Nabighian M N (1972), "The Analytic Signal Of Two-dimensional Magnetic Bodies With Polygonal Cross-section: Its Properties And Use For Automated Anomaly Interpretation, *Geophysics,* Vol. 37, pp. 507–517.
24. Nigerian Geological Survey Agency, (2006), "Geology Map of Nigeria", Scale1:2,00 000, Geology Survey of Nigeria, Kaduna, Nigeria.
25. Nwosu O B (2014), "Determination of Magnetic Basement Depth Over Parts of Middle Benue Trough By Source Parameter Imaging (SPI) Technique Using HRAM", *International Journal of Scientific & Technology Research* Vol. 3.
26. Obaje N G (2009), "Geology and mineral resources of Nigeria. Springer Dordrecht Heidelberg London New York.
27. Obiora S C (2009), "Field Measurements in Descriptions of Igneous and Metamorphic Rocks", in Lambert-Aikhionbare DO, Olayinka AI (Eds.), Proceedings of Field Mapping Standardisation Workshop, Ibadan University Press, Ibadan, pp. 105–125.
28. Ogezi A E O (1977), "Geochemistry and Geochronology of Basement Rocks from Northwestern Nigeria", Unpublished Ph.D. thesis Univ. leeds, England.

29. Parasnis D S (1986), *Principles of Applied Geophysics,* 4th Edition, Chapman and Hall, London, pp. 11-260.

30. Revees C (2005), "Aeromagnetic Surveys; Principles, Practice and Interpretation", GEOSOFT.

31. Russ W (1957), "The Geology of Parts of Niger, Zaria and Sokoto Provinces, with Special Reference to the Occurrence of Gold", *Geol. Surv. Nigeria, Bull*., No. 27.

32. Stanton R L (1972), *Ore Petrology*, McGraw-Hill Book Co., New York, pp. 419-443.

33. Telford W M, Geldart L P and Sheriff R E (1990), *Applied Geophysics*, Second Edition, Cambridge University Press.

34. Thurston and Smith (1997), "Automatic Conversion of Magnetic Data to Depth, Dip, and Susceptibility Contrast Using SPI Method", *Geophysics,* Vol. 62, pp. 807-813.

35. Thurston J, Smith R S and Guillion J C, (2002), A Multi-model Method for Depth Estimation from Magnetic Data", *Geophysics,* Vol. 67, pp. 555–561.

36. Thurston J, Guillion J C and Smith R S (1999), "Model- independent Depth Estimation with the SPI Method, *69th Annual International Meeting, SEG, Expanded Abstracts,* pp. 403–406.

37. Truswell J F and Cope R N (1963), "The geology of parts of Niger and Zaria Provinces, Northern Nigeria", *Geol Survey Nigeria Bull.,* Vol. 29, pp. 1–104.

38. Turner D C (1983), "Upper Proterozoic Schist Belts in the Nigerian Sector of the Pan African Province West Africa", *Precambrian Research*, Vol. 21, pp. 55-79.